Rapidity and Centrality Dependence of Proton and Anti-proton Production from ^{197}Au+^{197}Au Collisions at $\sqrt{s_{\rm NN}} = 130$ GeV

J. Adams,[3] C. Adler,[12] Aggarwal,[44] Z. Ahammed,[28] J. Amonett,[17] B.D. Anderson,[17] M. Anderson,[5] D. Arkhipkin,[11] G.S. Averichev,[10] S.K. Badyal,[45] J. Balewski,[13] O. Barannikova,[28,10] L.S. Barnby,[17] J. Baudot,[15] S. Bekele,[24] V.V. Belaga,[10] R. Bellwied,[41] J. Berger,[12] B.I. Bezverkhny,[43] S. Bhardwaj,[46] P. Bhaskar,[38] A.K. Bhati,[44] H. Bichsel,[40] A. Billmeier,[41] L.C. Bland,[2] C.O. Blyth,[3] B.E. Bonner,[30] M. Botje,[23] A. Boucham,[34] A. Brandin,[21] A. Bravar,[2] R.V. Cadman,[1] X.Z. Cai,[33] H. Caines,[43] M. Calderón de la Barca Sánchez,[2] A. Cardenas,[28] J. Carroll,[18] J. Castillo,[18] M. Castro,[41] D. Cebra,[5] P. Chaloupka,[9] S. Chattopadhyay,[38] H.F. Chen,[32] Y. Chen,[6] S.P. Chernenko,[10] M. Cherney,[8] A. Chikanian,[43] B. Choi,[36] W. Christie,[2] J.P. Coffin,[15] T.M. Cormier,[41] J.G. Cramer,[40] H.J. Crawford,[4] D. Das,[38] S. Das,[38] A.A. Derevschikov,[27] L. Didenko,[2] T. Dietel,[12] X. Dong,[32,18] J.E. Draper,[5] F. Du,[43] A.K. Dubey,[47] V.B. Dunin,[10] J.C. Dunlop,[2] M.R. Dutta Mazumdar,[38] V. Eckardt,[19] L.G. Efimov,[10] V. Emelianov,[21] J. Engelage,[4] G. Eppley,[30] B. Erazmus,[34] P. Fachini,[2] V. Faine,[2] J. Faivre,[15] R. Fatemi,[13] K. Filimonov,[18] P. Filip,[9] E. Finch,[43] Y. Fisyak,[2] D. Flierl,[12] K.J. Foley,[2] J. Fu,[18,42] C.A. Gagliardi,[35] M.S. Ganti,[38] T.D. Gutierrez,[5] N. Gagunashvili,[10] J. Gans,[43] L. Gaudichet,[34] M. Germain,[15] F. Geurts,[30] V. Ghazikhanian,[6] P. Ghosh,[38] J.E. Gonzalez,[6] O. Grachov,[41] V. Grigoriev,[21] D. Grosnick,[37] M. Guedon,[15] S.M. Guertin,[6] A. Gupta,[45] E. Gushin,[21] T.J. Hallman,[2] D. Hardtke,[18] J.W. Harris,[43] M. Heinz,[43] T.W. Henry,[35] S. Heppelmann,[26] T. Herston,[28] B. Hippolyte,[43] A. Hirsch,[28] E. Hjort,[18] G.W. Hoffmann,[36] M. Horsley,[43] H.Z. Huang,[6] S.L. Huang,[32] T.J. Humanic,[24] G. Igo,[6] A. Ishihara,[36] P. Jacobs,[18] W.W. Jacobs,[13] M. Janik,[39] I. Johnson,[18] P.G. Jones,[3] E.G. Judd,[4] S. Kabana,[43] M. Kaneta,[18] M. Kaplan,[7] D. Keane,[17] J. Kiryluk,[6] A. Kisiel,[39] J. Klay,[18] S.R. Klein,[18] A. Klyachko,[13] D.D. Koetke,[37] T. Kollegger,[12] A.S. Konstantinov,[27] M. Kopytine,[17] L. Kotchenda,[21] A.D. Kovalenko,[10] M. Kramer,[22] P. Kravtsov,[21] K. Krueger,[1] C. Kuhn,[15] A.I. Kulikov,[10] A. Kumar,[44] G.J. Kunde,[43] C.L. Kunz,[7] R.Kh. Kutuev,[11] A.A. Kuznetsov,[10] M.A.C. Lamont,[3] J.M. Landgraf,[2] S. Lange,[12] C.P. Lansdell,[36] B. Lasiuk,[43] F. Laue,[2] J. Lauret,[2] A. Lebedev,[2] R. Lednický,[10] V.M. Leontiev,[27] M.J. LeVine,[2] C. Li,[32] Q. Li,[41] S.J. Lindenbaum,[22] M.A. Lisa,[24] F. Liu,[42] L. Liu,[42] Z. Liu,[42] Q.J. Liu,[40] T. Ljubicic,[2] W.J. Llope,[30] H. Long,[6] R.S. Longacre,[2] M. Lopez-Noriega,[24] W.A. Love,[2] T. Ludlam,[2] D. Lynn,[2] J. Ma,[6] Y.G. Ma,[33] D. Magestro,[24] S. Mahajan,[45] L.K. Mangotra,[45] A.P. Mahapatra,[47] R. Majka,[43] R. Manweiler,[37] S. Margetis,[17] C. Markert,[43] L. Martin,[34] J. Marx,[18] H.S. Matis,[18] Yu.A. Matulenko,[27] T.S. McShane,[8] F. Meissner,[18] Yu. Melnick,[27] A. Meschanin,[27] M. Messer,[2] M.L. Miller,[43] Z. Milosevich,[7] N.G. Minaev,[27] C. Mironov,[17] D. Mishra,[47] J. Mitchell,[30] B. Mohanty,[38] L. Molnar,[28] C.F. Moore,[36] M.J. Mora-Corral,[19] V. Morozov,[18] M.M. de Moura,[41] M.G. Munhoz,[31] B.K. Nandi,[38] S.K. Nayak,[45] T.K. Nayak,[38] J.M. Nelson,[3] P. Nevski,[2] V.A. Nikitin,[11] L.V. Nogach,[27] B. Norman,[17] S.B. Nurushev,[27] G. Odyniec,[18] A. Ogawa,[2] V. Okorokov,[21] M. Oldenburg,[18] D. Olson,[18] G. Paic,[24] S.U. Pandey,[41] S. Pal,[38] Y. Panebratsev,[10] S.Y. Panitkin,[2] A.I. Pavlinov,[41] T. Pawlak,[39] V. Perevoztchikov,[2] W. Peryt,[39] V.A. Petrov,[11] S.C. Phatak,[47] R. Picha,[5] J. Pluta,[39] N. Porile,[28] J. Porter,[2] A.M. Poskanzer,[18] M. Potekhin,[2] E. Potrebenikova,[10] B.V.K.S. Potukuchi,[45] D. Prindle,[40] C. Pruneau,[41] J. Putschke,[19] G. Rai,[18] G. Rakness,[13] R. Raniwala,[46] S. Raniwala,[46] O. Ravel,[34] R.L. Ray,[36] S.V. Razin,[10,13] D. Reichhold,[28] J.G. Reid,[40] G. Renault,[34] F. Retiere,[18] A. Ridiger,[21] H.G. Ritter,[18] J.B. Roberts,[30] O.V. Rogachevski,[10] J.L. Romero,[5] A. Rose,[41] C. Roy,[34] L.J. Ruan,[32,2] V. Rykov,[41] R. Sahoo,[47] I. Sakrejda,[18] S. Salur,[43] J. Sandweiss,[43] I. Savin,[11] J. Schambach,[36] R.P. Scharenberg,[28] N. Schmitz,[19] L.S. Schroeder,[18] K. Schweda,[18] J. Seger,[8] D. Seliverstov,[21] P. Seyboth,[19] E. Shahaliev,[10] M. Shao,[32] M. Sharma,[44] K.E. Shestermanov,[27] S.S. Shimanskii,[10] R.N. Singaraju,[38] F. Simon,[19] G. Skoro,[10] N. Smirnov,[43] R. Snellings,[23] G. Sood,[44] P. Sorensen,[6] J. Sowinski,[13] H.M. Spinka,[1] B. Srivastava,[28] S. Stanislaus,[37] E.J. Stephenson,[13] R. Stock,[12] A. Stolpovsky,[41] M. Strikhanov,[21] B. Stringfellow,[28] C. Struck,[12] A.A.P. Suaide,[41] E. Sugarbaker,[24] C. Suire,[2] M. Šumbera,[9] B. Surrow,[2] T.J.M. Symons,[18] A. Szanto de Toledo,[31] P. Szarwas,[39] A. Tai,[6] J. Takahashi,[31] A.H. Tang,[2,23] P. Sorensen,[48] D. Thein,[6] J.H. Thomas,[18] V. Tikhomirov,[21] M. Tokarev,[10] M.B. Tonjes,[20] T.A. Trainor,[40] S. Trentalange,[6] R.E. Tribble,[35] M.D. Trivedi,[38] V. Trofimov,[21] O. Tsai,[6] T. Ullrich,[2] D.G. Underwood,[1] G. Van Buren,[2] A.M. VanderMolen,[20] A.N. Vasiliev,[27] M. Vasiliev,[35] S.E. Vigdor,[13] Y.P. Viyogi,[38] S.A. Voloshin,[41] F. Wang,[28] G. Wang,[17] X.L. Wang,[32] Z.M. Wang,[32] H. Ward,[36] J.W. Watson,[17] R. Wells,[24] G.D. Westfall,[20] C. Whitten Jr.,[6] H. Wieman,[18] R. Willson,[24] S.W. Wissink,[13] R. Witt,[43] J. Wood,[6] J. Wu,[32] N. Xu,[18] Z. Xu,[2] Z.Z. Xu,[32] A.E. Yakutin,[27] E. Yamamoto,[18] J. Yang,[6] P. Yepes,[30] V.I. Yurevich,[10] Y.V. Zanevski,[10] I. Zborovský,[9] H. Zhang,[43,2] H.Y. Zhang,[17] W.M. Zhang,[17] Z.P. Zhang,[32] P.A. Żołnierczuk,[13] R. Zoulkarneev,[11] J. Zoulkarneeva,[11] and A.N. Zubarev[10]

[1] *Argonne National Laboratory, Argonne, Illinois 60439*

[2]Brookhaven National Laboratory, Upton, New York 11973
[3]University of Birmingham, Birmingham, United Kingdom
[4]University of California, Berkeley, California 94720
[5]University of California, Davis, California 95616
[6]University of California, Los Angeles, California 90095
[7]Carnegie Mellon University, Pittsburgh, Pennsylvania 15213
[8]Creighton University, Omaha, Nebraska 68178
[9]Nuclear Physics Institute AS CR, Řež/Prague, Czech Republic
[10]Laboratory for High Energy (JINR), Dubna, Russia
[11]Particle Physics Laboratory (JINR), Dubna, Russia
[12]University of Frankfurt, Frankfurt, Germany
[13]Indiana University, Bloomington, Indiana 47408
[14]Insitute of Physics, Bhubaneswar 751005, India
[15]Institut de Recherches Subatomiques, Strasbourg, France
[16]University of Jammu, Jammu 180001, India
[17]Kent State University, Kent, Ohio 44242
[18]Lawrence Berkeley National Laboratory, Berkeley, California 94720
[19]Max-Planck-Institut fuer Physik, Munich, Germany
[20]Michigan State University, East Lansing, Michigan 48824
[21]Moscow Engineering Physics Institute, Moscow Russia
[22]City College of New York, New York City, New York 10031
[23]NIKHEF, Amsterdam, The Netherlands
[24]Ohio State University, Columbus, Ohio 43210
[25]Panjab University, Chandigarh 160014, India
[26]Pennsylvania State University, University Park, Pennsylvania 16802
[27]Institute of High Energy Physics, Protvino, Russia
[28]Purdue University, West Lafayette, Indiana 47907
[29]University of Rajasthan, Jaipur 302004, India
[30]Rice University, Houston, Texas 77251
[31]Universidade de Sao Paulo, Sao Paulo, Brazil
[32]University of Science & Technology of China, Anhui 230027, China
[33]Shanghai Institute of Nuclear Research, Shanghai 201800, P.R. China
[34]SUBATECH, Nantes, France
[35]Texas A & M, College Station, Texas 77843
[36]University of Texas, Austin, Texas 78712
[37]Valparaiso University, Valparaiso, Indiana 46383
[38]Variable Energy Cyclotron Centre, Kolkata 700064, India
[39]Warsaw University of Technology, Warsaw, Poland
[40]University of Washington, Seattle, Washington 98195
[41]Wayne State University, Detroit, Michigan 48201
[42]Institute of Particle Physics, CCNU (HZNU), Wuhan, 430079 China
[43]Yale University, New Haven, Connecticut 06520
[44]Panjab University, Chandigarh, 160014, India
[45]University of Jammu, Jammu, 180001, India
[46]University of Rajasthan, Jaipur, 302004, India
[47]Insitute of Physics, Bhubaneswar, 751005, India
[48]University of California, Los Angeles,California 90095

(Dated: June 20, 2003)

We report on the rapidity and centrality dependence of proton and anti-proton transverse mass distributions from ^{197}Au+^{197}Au collisions at $\sqrt{s_{\rm NN}} = 130$ GeV as measured by the STAR experiment at RHIC. Our results are from the rapidity and transverse momentum range of $|y| < 0.5$ and $0.35 < p_t < 1.00$ GeV/c. For both protons and anti-protons, transverse mass distributions become more convex from peripheral to central collisions demonstrating characteristics of collective expansion. The measured rapidity distributions and the mean transverse momenta versus rapidity are flat within $|y| < 0.5$. Comparisons of our data with results from model calculations indicate that in order to obtain a consistent picture of the proton(anti-proton) yields and transverse mass distributions the possibility of pre-hadronic collective expansion may have to be taken into account.

High energy nuclear collisions provide a unique opportunity to study matter under extreme conditions for which one expects the formation of a system dominated by deconfined quarks and gluons [1]. In the search for this deconfined state, baryons play an important role. Incoming beam baryons provide the energy for particle production and development of collective motion. It has systematically been observed that the net-baryon num-

ber determines the chemical properties [2]. In addition, baryon transport and baryon production during the collision are particularly interesting because of their dynamical nature [3, 4, 5, 6, 7, 8]. However, these are difficult processes due to their non-perturbative features [9, 10]. At the RHIC energy $\sqrt{s_{\rm NN}}$ =130 GeV, anti-proton to proton ratios and yields at mid-rapidity have been reported by several experiments [11, 12, 13, 14]. In the region of $p_t \sim$ 2-3 GeV/c, the yield of protons approaches that of pions [12] in central collisions. The exact origin of this behavior is not clear and systematic measurements of baryon distributions are important.

In this Letter, we present a systematic measurement of proton and anti-proton production in Au+Au collisions at $\sqrt{s_{NN}} = 130$ GeV in the rapidity range $-0.5 < y < 0.5$ and for transverse momenta $0.35 < p_t < 1.00$ GeV/c. In particular, we report the first RHIC measurements of the rapidity dependence of the proton and anti-proton yields, essential for exploring the existence of a boost-invariant region in the system. We also study the centrality dependence of the yields and mean transverse momenta for protons and anti-protons. These results allow for a detailed comparison to model predictions of proton and anti-proton production at RHIC.

Two independent ^{197}Au beams with an energy of 65 GeV per nucleon were provided by the Relativistic Heavy Ion Collider (RHIC) at the Brookhaven National Laboratory. These beams collided around the geometric center of the Solenoid Tracker at RHIC (STAR). Charged particles stemming from these collisions were measured in a large volume Time Projection Chamber (TPC) [15]. A large solenoidal magnet of 0.25 T field strength provided momentum dispersion in the direction transverse to the beam line.

For this analysis, we used 320k events with a minimum bias trigger and 154k events with a trigger selecting the 10% most central events [11]. Events with a primary vertex within ±30 cm of the geometric center of the TPC along the beam axis were accepted. Tracks were required to have at least 23 out of 45 maximum possible space points in the TPC and to extrapolate back to the primary vertex within 2 cm (distance of closest approach, *dca*). To define the collision centrality, the measured raw multiplicity distribution of charged particles within the pseudorapidity range $|\eta| < 0.75$ was divided into eight bins. The highest centrality bin corresponds to 6% of the measured cross section for ^{197}Au+^{197}Au collisions [16]. Protons and anti-protons were identified by correlating their energy loss dE/dx due to ionization in the TPC gas with the measured momentum. This method has already been presented in [11].

The track reconstruction efficiency was determined by embedding simulated tracks into real events at the raw data level and subsequently applying the full reconstruction algorithm to those events. The propagation of single tracks was performed using the GEANT Monte Carlo code with a detailed model of the STAR geometry and a realistic simulation of the TPC response. The resulting track reconstruction efficiency is $> 70\%$ at $p_t > 0.5$ GeV/c for all centralities. By varying the track cuts, the overall systematic uncertainty in the track reconstruction efficiency is estimated to be less than 10%. Further, the relative resolution in transverse momentum was derived to be $\approx 4\%$ at $p_t = 0.5$ GeV/c.

Secondary interactions of particles with the detector material generated background protons. Due to their different geometric origin, these background protons appear as a rather flat tail in the *dca*-distribution which extends into the peak region of primary protons at small *dca*. In order to correct for background protons, the proton *dca*–distribution was fitted by the scaled anti-proton *dca*–distribution (which is background free) plus the results on the proton background from Monte Carlo calculations. Raw yields were extracted for protons and anti-protons with $dca < 2.0$ cm, optimizing the signal to background ratio for protons. The raw yields were then corrected for track reconstruction efficiency, proton background and in the case of anti-protons, for absorption in the detector material. The detector acceptance for protons(anti-protons) from the decay of lambdas(anti-lambdas) or other hyperons(anti-hyperons) is estimated to be larger than 95%. Corrections for feeddown from decays of hyperons(anti-hyperons) were not applied.

The mid-rapidity ($|y| \leq 0.5$) proton and anti-proton transverse mass distributions for all 8 centrality bins are shown in Fig. 1. Here, the transverse mass m_t is given by $m_t = \sqrt{p_t^2 + m_p^2}$, with m_p the rest mass of the proton. The uncorrelated bin-to-bin systematic errors are estimated to be less than 7%. It is evident that both proton (left panel) and anti-proton (right panel) distributions become more convex from peripheral to central collisions indicating an increase in transverse radial flow. In order to extract p_t-integrated yields, dN/dy and mean transverse momenta $\langle p_t \rangle$, hydrodynamically motivated fits [17] were applied, assuming a thermal source plus transverse radial flow. The fit parameters are the temperature T_{fo} at kinetic freeze-out and the transverse radial flow velocity β_s at the system surface. A velocity profile $\beta_t(r) = \beta_s(r/R)^{0.5}$ was used, where R is the radius of the source. These fits simultaneously describe experimental spectra of charged pions [18], kaons [19], protons and anti-protons. The fit-results are shown as dashed lines in Fig. 1. The description of the experimental data is remarkably good. When strong collective flow develops, the transverse mass distributions for heavy mass particles will not have the simple exponential shape at low transverse mass. Therefore, the hydrodynamically motivated two parameter fits become necessary [20]. The increase of $\langle p_t \rangle$ with centrality is indeed reflected in the values of the collective velocity parameter $\langle \beta_t \rangle$, which increase from about $(0.42 \pm 0.10)c$ to $(0.56 \pm 0.05)c$ from the most peripheral to the most central collisions, respectively.

Note that in [11], the anti-proton transverse momentum distributions were fitted with a Gaussian function in p_t. The difference between the model fit results and Gaussian fits in p_t are $< 6\%$ and $< 10\%$ for $\langle p_t \rangle$ and inte-

grated yields dN/dy, respectively. Using other functions, i.e. exponential in m_t and a Boltzmann function, the systematic uncertainty in dN/dy due to extrapolation is estimated to be less than 20%. Similarly, the systematic uncertainty in $\langle p_t \rangle$ is less than 6%. The total systematic uncertainty in dN/dy is less than 22%, adding the contributions due to extrapolation (20%) and the track reconstruction efficiency (10%) in quadrature. The proton and anti-proton rapidity distributions are shown in Fig. 2 (a) and (b) for different collision centralities. In the p_t-range not covered by this experiment, the yield was extracted from the thermal model fit. The results are shown in Table I, which indicates that about 50% of the integrated yield was measured within the STAR TPC acceptance. The bin-to-bin systematic errors, due to background subtraction and PID contamination, are included in the plot. Since the shapes of the transverse mass distributions of protons and anti-protons do not differ within statistical errors, the extracted values of $\langle p_t \rangle$ shown in Fig. 2(c) are the average of the two. Within $|y| < 0.5$, both values of $\langle p_t \rangle$ and dN/dy are found to be uniform as a function of rapidity indicating that at RHIC – for the first time in heavy ion collisions – a boost invariant region of at least one unit of rapidity for all centrality bins has developed. An analysis of charged particle ratios [21] has demonstrated that at RHIC energies a boost invariant region does not exist at $|y| > 1.5$. It will be of interest to study the rapidity distributions of different mass hadrons at RHIC.

The top panels of Figure 3 show the $\langle p_t \rangle$ within $|y| \leq 0.5$ for protons (left) and anti-protons (right). The corresponding yields, dN/dy are shown in the bottom panels. The open symbols represent fiducial yields and filled ones show the integrated yields. The shaded bands indicate the systematic uncertainties in extracting $\langle p_t \rangle$ and dN/dy. Both values of $\langle p_t \rangle$ and dN/dy are in good agreement with results from PHENIX [12]. Experimental results on the lambda(anti-lambda) yields [22], show that the contribution of feeddown from hyperon decays to the proton(anti-proton) yields is ≈40%. The increase of $\langle p_t \rangle$ vs. centrality in the figure indicates the development of stronger collective expansion in more central collisions. Results from calculations with RQMD [23], RQMD with re-scattering switched off (w/o) and HIJING [24, 25] are represented by solid, dashed, and dashed-dotted lines, respectively. In the RQMD model [23, 26] hadronic re-scattering has been implemented. This leads to the agreement with measurements in the mean transverse momentum. On the other hand, without the re-scattering, the HIJING model under-predicts the proton and anti-proton $\langle p_t \rangle$, especially for central collisions. Overall, the model calculations fail to predict the experimental yields consistently throughout the whole centrality range. Discrepancies between measured $\overline{p}/p$ ratios and predictions from RQMD and HIJING have been reported by other experiments [13, 14].

The bottom panels of Fig. 3 show that the observed mid-rapidity ($|y| \leq 0.5$) proton and anti-proton yields, dN/dy are proportional to the number of charged hadrons. RQMD fails to predict the centrality dependence of the anti-proton yield due to the strong annihilation in hadronic re-scattering, especially in central collisions. Because of the annihilation, RQMD predicts a change in the $\overline{p}/p$ ratio of almost a factor of two from peripheral to central collisions, which is not consistent with observations [11].

The results from RQMD reflect that within that model there is strong annihilation among baryons, and that large values of $\langle p_t \rangle$ are built up from late hadronic rescatterings. Based on RQMD, the annihilation of anti-protons created initially is expected to increase from 20% for perpiheral collisions, to 50% for the most central collisions. This is not consistent with the trend in Fig. 3, which indicates the measured proton and anti-proton yields increase approximately linearly with the number of negatively charged hadrons. This raises an important question. If, on the one hand the increase in annihilation with centrality predicted by RQMD is correct, then the centrality dependence of the initial baryon production must be much stronger than the linear dependence observed in Fig. 3, and the rough agreement between RQMD and the data for anti-protons is fortuitous. If, on the other hand, the agreement between RQMD and the linear dependence observed in Fig. 3 for anti-protons is correct, a possible explanation is that the anti-proton loss due to annihilation is smaller in central collisions than in peripheral collisions. This suggests the anti-protons may decouple from the surrounding matter early, and that the large experimental values of $\langle p_t \rangle$ which are observed must arise from collective flow in the early stage [27, 28, 29]. In order to distinguish this possibility from other possible scenarios [30] and study possible early-stage partonic collectivity at RHIC, systematic measurements of multi-strange baryons, charmed mesons, and particle correlations are necessary.

In summary, we have reported on the centrality dependence of proton and anti-proton transverse mass and rapidity distributions from ^{197}Au+^{197}Au collisions at $\sqrt{s_{\rm NN}} = 130$ GeV as measured by the STAR experiment at RHIC. The results reported here are from the rapidity and transverse momentum range of $|y| < 0.5$ and $0.35 < p_t < 1.00$ GeV/c. For both protons and anti-protons, the transverse mass distributions become more convex from peripheral to central collisions indicating the enhancement of collective expansion in more central collisions. The rapidity distributions and $\langle p_t \rangle$ versus rapidity are found to be flat within $|y| < 0.5$ suggesting a boost invariant region around mid-rapidity. The comparison of our data to results from microscopic transport models suggests that the observed collective expansion might have been dominantly developed at the early stage of the collision.

We thank Drs. W. Busza, M. Gyulassy and V. Topor-Pop for exciting discussions. We wish to thank the RHIC Operations Group at Brookhaven National Laboratory

TABLE I: Mid-rapidity ($|y| < 0.5$) proton and anti-proton results on $\langle p_t \rangle$ and rapidity densities. The fiducial yield is measured within $0.35 < p_t < 1.00$ GeV/c. The errors are statistical. See text for discussions of systematic errors.

Cent. bin	$\langle p_t \rangle$ (MeV)	dN_p/dy (fiducial)	dN_p/dy (integrated)	$dN_{\overline{p}}/dy$ (fiducial)	$dN_{\overline{p}}/dy$ (integrated)
58–85%	738±6	0.98±0.01	1.62±0.02	0.78±0.01	1.28±0.01
45–58%	805±6	2.51±0.02	4.36±0.05	1.91±0.02	3.31±0.03
34–45%	856±6	3.96±0.03	7.14±0.08	2.97±0.02	5.35±0.06
26–34%	892±6	5.55±0.04	10.29±0.10	4.08±0.03	7.56±0.07
18–26%	883±7	7.16±0.05	13.03±0.11	5.22±0.03	9.50±0.09
11–18%	900±8	8.92±0.06	16.53±0.14	6.40±0.04	11.85±0.10
6–11%	945±8	10.72±0.04	21.01±0.19	7.67±0.02	15.04±0.14
0– 6%	965±7	13.17±0.04	26.37±0.23	9.35±0.02	18.72±0.16

for their tremendous support and for providing collisions for the experiment. This work was supported by the Division of Nuclear Physics and the Division of High Energy Physics of the Office of Science of the U.S. Department of Energy, the United States National Science Foundation, the Bundesministerium für Bildung und Forschung of Germany, the Institut National de la Physique Nucleaire et de la Physique des Particules of France, the United Kingdom Engineering and Physical Sciences Research Council, Fundacao de Amparo a Pesquisa do Estado de Sao Paulo, Brazil, the Russian Ministry of Science and Technology, the Ministry of Education of China and the National Natural Science Foundation of China.

[1] For reviews and recent developments see Nucl. Phys. **A698**, 1c(2002).
[2] P. Braun-Munzinger, D. Magestro, K. Redlich, and J. Stachel, Phys. Lett. **B518**, 41(2001).
[3] W. Busza and R. Ledoux, Annu. Rev. Nucl. Part. Sci. **38**, 119(1988).
[4] F. Videbaek and O. Hansen, Phys. Rev. **C52**, 2684(1995).
[5] J. Barrette *et al.* (E814 Collaboration), Z. Physik **C59**, 211(1993).
[6] L. Ahle *et al.* (E802 Collaboration), Phys. Rev. Lett. **81**, 2650(1998).
[7] I.G. Bearden *et al.* (NA44 Collaboration), Phys. Lett. **B388**, 431(1996); I.G. Bearden *et al.* (NA44 Collaboration), Phys. Rev. **C66**, 044907(2002).
[8] H. Appelshäuser *et al.* (NA49 Collaboration), Phys. Rev. Lett. **82**, 2471(1999).
[9] S. Daté, M. Gyulassy, and H. Sumiyoshi, Phys. Rev. **D32**, 619(1985).
[10] I.N. Mishustin and J.I. Kapusta, Phys. Rev. Lett. **88**, 112501(2002).
[11] C. Adler *et al.* (STAR Collaboration), Phys. Rev. Lett. **86**, 4778(2001); *ibid.* **87**, 262302(2001); *ibid.* **90**, 119903(E)(2003).
[12] K. Adcox *et al.*, (PHENIX Collaboration), Phys. Rev. Lett. **88**, 242301(2002)
[13] I.G. Bearden *et al.* (BRAHMS Collaboration) Phys. Rev. Lett. **87**, 112305(2002).
[14] B.B. Back *et al.*, (PHOBOS Collaboration), Phys. Rev. Lett. **87**, 102301(2001).
[15] H. Wieman *et al.*, IEEE Trans. Nucl. Sci. **44**, 671(1997); W. Betts *et al.*, IEEE Trans. Nucl. Sci. **44**, 592(1997); S. Klein *et al.*, IEEE Trans. Nucl. Sci. **43**, 1768(1996).
[16] K.H. Ackermann *et al.* (STAR Collaboration), Phys. Rev. Lett. **86**, 402(2001).
[17] E. Schnedermann, J. Sollfrank, and U. Heinz, Phys. Rev. **C48**, 2462(1993).
[18] M. Calderón de la Barca Sánchez, *et al.* (STAR Collaboration), Nucl. Phys. **A698**, 503c(2002); M. Calderón de la Barca Sánchez, Ph.D. Thesis, Yale University, USA(2001).
[19] C. Adler *et al.* (STAR Collaboration), subm. to Phys. Lett. **B**; nucl-ex/0206008.
[20] I.G. Bearden *et al.* (NA44 Collaboration), Phys. Rev. Lett. **78**, 2080(1997).
[21] I.G. Bearden *et al.* (BRAHMS Collaboration), Phys. Rev. Lett. **90**, 102301(2003).
[22] C. Adler *et al.* (STAR Collaboration), Phys. Rev. Lett. **89**, 092301(2002).
[23] H. Sorge, Phys. Rev. **C52**, 3291(1995).
[24] X.N. Wang, Phys. Rep. **280**, 287(1997).
[25] S.E. Vance, M. Gyulassy, and X.N. Wang, Phys. Lett. **B443**, 45(1998); S.E. Vance, Nucl. Phys. **A661**, 230c(1999).
[26] B. Monreal *et al.*, Phys. Rev. **C60**, R031901(1999); *ibid.* R051902(1999).
[27] L. McLerran and J. Schaffner-Bielich, Phys. Lett. **B514**, 29(2001).
[28] C. Adler *et al.* (STAR Collaboration), Phys. Rev. Lett. **87**, 112303(2001); *ibid.* **89**, 132301(2002); C. Adler *et al.* (STAR Collaboration), Phys. Rev. **C66**, 034904 (2002).
[29] C. Adler *et al.* (STAR Collaboration), Phys. Rev. Lett. **90**, 082302(2003).
[30] R. Rapp and E. Shuryak, Nucl. Phys. **A698**, 587c(2002).

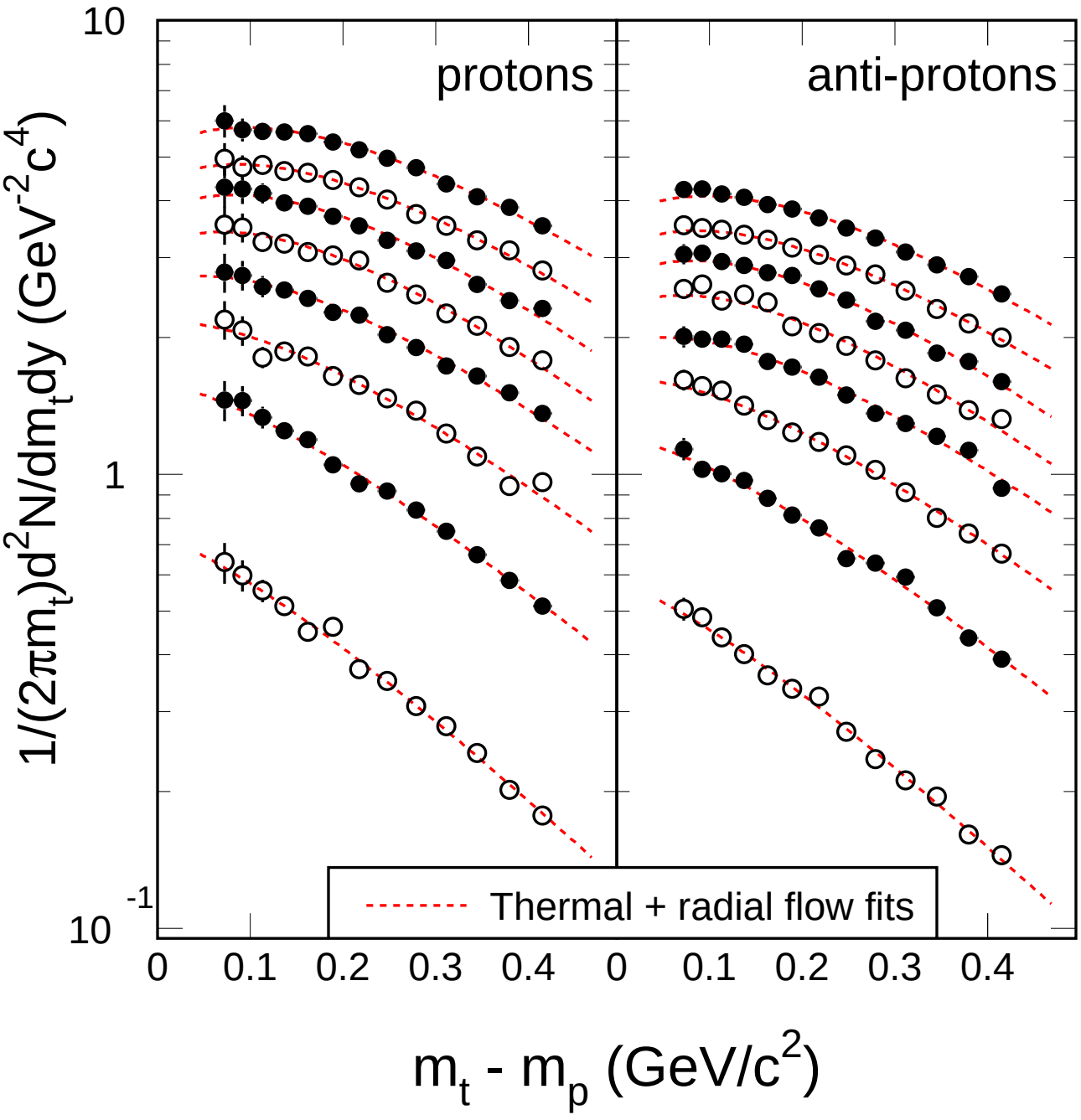

FIG. 1: Mid-rapidity ($|y| \leq 0.5$) proton (left column) and anti-proton (right column) transverse mass distributions for most peripheral (bottom) to most central (top) collisions. The definitions of the centrality bins are listed in Table I. Relatively large systematic errors for protons in the low m_t region are due to the background subtraction. Results from model fits are shown as dashed lines.

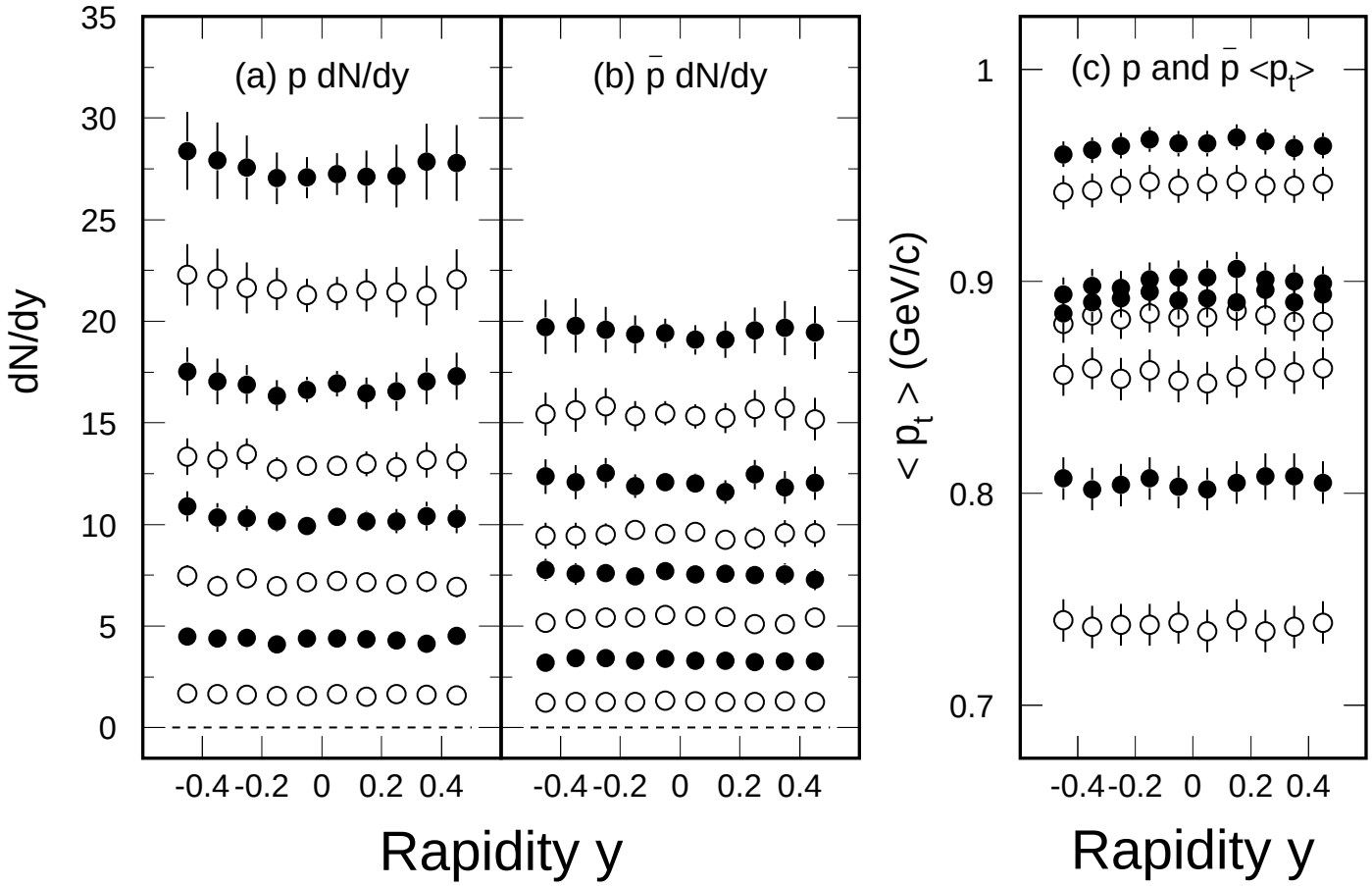

FIG. 2: The rapidity distributions of protons (a) and anti-protons (b) and the average transverse momentum $\langle p_t \rangle$ (c), for most peripheral (bottom) to most central (top) collisions. The bin-to-bin systematic errors due to PID contamination, were included in the plot. Overall systematic errors due to extrapolation into the p_t-range not covered by the experiment and the uncertainty in the track reconstruction efficiency are not shown in the figure.

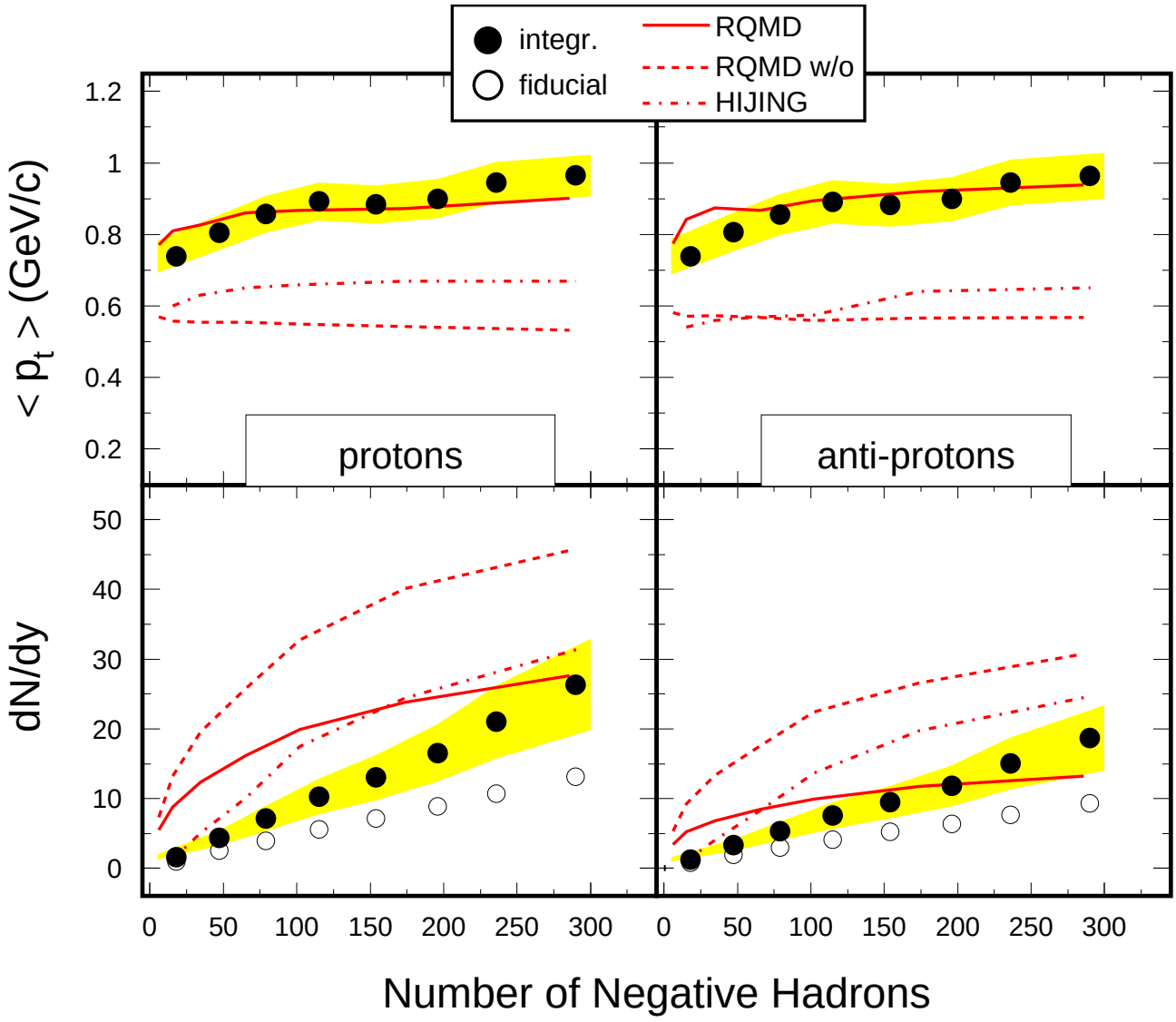

FIG. 3: Mid-rapidity $\langle p_t \rangle$ and dN/dy of protons and anti-protons as functions of the number of negatively charged hadrons. Open symbols are fiducial yields and filled ones are integrated yields. Systematic errors in the integrated yields are shown as shaded areas. Results from RQMD, RQMD with re-scattering switched off (w/o) and HIJING are shown as solid-lines, dashed-lines and dashed-dotted lines respectively. The experimental data and the results from RQMD and HIJING include feeddown from hyperon decay.